Low pressure characterization of dielectric barrier discharge actuators

Jignesh Soni and Subrata Roy[a)]
Applied Physics Research Group, Department of Mechanical and Aerospace Engineering, University of Florida, Gainesville, Florida 32611, USA

(Received 2 January 2013; accepted 8 March 2013; published online 20 March 2013)

Dielectric barrier discharge actuators tested for thrust inducement between 13 and 101 kPa ambient air pressure show that as the pressure decreases, the thrust increases to a maximum, then drops steadily approaching zero while the power consumption monotonically increases. The amplification in induced thrust at the peak ranges from a few percent to several folds of the thrust measured at atmospheric condition. The effect is more pronounced for thinner dielectrics at lower operating voltages than thicker dielectrics at higher operating voltages and is fairly independent of the ground electrode width. Results identify several optimal control parameters for high-altitude operations. © *2013 American Institute of Physics*. [http://dx.doi.org/10.1063/1.4796176]

Dielectric barrier discharge (DBD) actuators offer unique flow control advantages over rival technologies, such as lack of moving parts, scalability, versatility of design and geometry, and surface compliance. They work by locally injecting momentum into the boundary layer to delay/avoid separation, or alter the shape and characteristics of the flow. Early results found that these devices induced wall jets along the surface of the dielectric.[1] Since then, extensive work has been carried out characterizing the performance of these actuators with respect to geometry, electrical parameters, dielectric properties, and underlying physics.[2–6] While a broad range of control parameters are well understood,[7,8] the effect of operating pressure is yet to be fully explored. A theoretical model,[9] complemented with experimental results between a pressure range of 18 to 78 kPa, suggested a linear decrease in thrust with neutral gas density at constant power. However, when the pressure was reduced from atmospheric (101 kPa) condition at constant voltage, the induced thrust first increased to a slightly (~10%) higher value at around 80 kPa, followed by a gradual decay with pressure.[10]

A recent study[11] focused on the average initiation voltage as a function of dielectric material and thickness. The dielectric capacitance based on these two parameters was found to have a negative power relationship with the average initiation voltage at any given pressure between 50 and 810 kPa. For a given capacitance, the initiation voltage was found to increase with increasing pressure. Within the same paper, the authors mentioned about an unpublished work (Fig. 12 in Ref. 11) on the variation of induced thrust for a 2.28 mm glass actuator that confirmed similar trend[10] in measured thrust between a pressure range of 23 to 99 kPa. The increase in force was found to be more pronounced at higher voltages. The pressure at which the force reached a maximum was found to be a function of the operating voltage, with higher operating voltages leading to the thrust peaking at lower pressures. However, at lower voltages (<22.6 kVpp), the thrust reduced continually without a discernible local maxima.

Another study[12] between a pressure range of 101 and 342 kPa demonstrated significant reduction in the induced velocity and body force at elevated pressures. An increase in ambient air temperature from 30 to 200 °C at atmospheric pressure resulted in an almost linear increase in the induced body force, reaching about twice the nominal value at the highest temperature.

The present work is undertaken with the aim of understanding the performance of plasma actuators for a broader range of control parameters (operating pressure, dielectric thickness, dielectric material, and applied voltage) under sub-atmospheric pressures. The physical influence of these parameters on thrust generation has been investigated by discovering parametric relationships grounded in experiments. Since plasma generation itself is a strong function of pressure, one may expect a mutual correlation among other quantities, with pressure as the unifying parameter.

The actuators tested in this letter have varying lengths, necessitating two different setups for reliable thrust measurement. Figure 1 shows the general experimental setup. For measuring thrust from relatively long actuators (30 cm length), a commercial high precision electronic balance (Ohaus Adventure Pro™ AV313C) with a resolution of 1 mg is used (Figure 1(a)). The balance is placed in an acrylic vacuum chamber (60 cm × 30 cm × 30 cm), connected to a vacuum pump via a relief valve used to regulate the level of vacuum. A pressure gauge (MKS 910 Piezo Pirani) fitted to the side of the chamber reads the pressure to within 1% error.

Figure 1(b) shows the setup for a torsion balance based micro-Newton thrust stand (μNTS) built specifically for measuring thrusts smaller than the resolution of the commercial balance. Similar devices have been reported in literature.[13] Two flexure pivots at the vertical ends of a cross-beam form the torsion spring. A pair of aluminum disc electrodes provides a known thrust or a controlled displacement for calibration. An optical linear displacement sensor (Philtec Model D-63) measures the displacement of the balance arm at a distance to calculate the angular deflection. The actuator is mounted horizontally at one end of the crossbeam for taking measurements.

To facilitate quick readings and reduce the noise floor, a magnetic damper is introduced based on eddy current damping, as shown in Figure 2(a). A cylindrical copper block

a)Author to whom correspondence should be addressed. Electronic mail: roy@ufl.edu. URL: http://aprg.mae.ufl.edu/roy/.

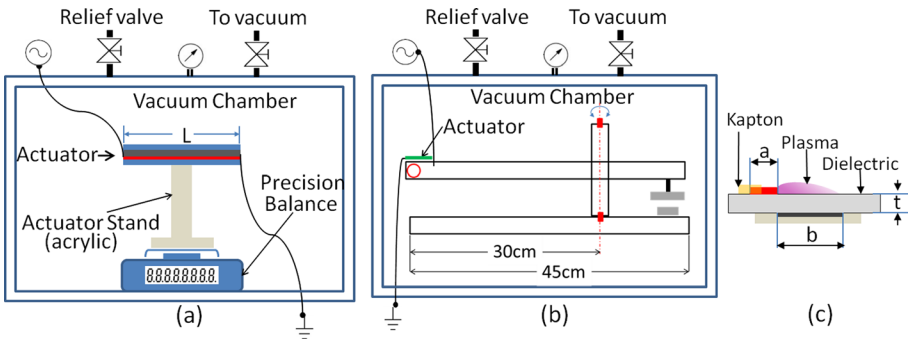

FIG. 1. Experimental setup inside vacuum chamber: (a) commercial precision balance, (b) custom thrust stand, (c) typical actuator configuration.

(6.35 cm diameter × 2.5 cm height) of high conductivity is mounted on the balance arm, with a permanent magnet placed under it in close proximity. The relative motion of the copper block and the magnet induces eddy currents in the block, which generate their own magnetic field, counter to the applied magnetic field. The applied and induced magnetic fields interact to produce a force proportional to the relative motion, essentially providing damping. Magnetic damping has inherent advantages of being a non-contact damper (as opposed to a viscous damper) and non-powered (as opposed to an electromagnetic/electrostatic damper). Figure 2(b) describes the system response demonstrating how close-to-critical damping may be achieved by controlling the gap between the copper block and the permanent magnet.

The system is calibrated using the electrostatic force method, as well as the logarithmic decrement method, for robustness and redundancy. Calibration values from both the electrostatic force and the log decrement methods converge around 0.00345 Nm/deg (plot not shown for brevity). Thrust measurement from the μNTS is compared with the commercial balance using a test actuator and is found to be in good agreement (within 10%). The statistical scatter in the calibration constant is seen to be around 20% which is considered as the error margin for μNTS data measurement. Zito *et al.*[14] have demonstrated the use of the μNTS for direct thrust measurement of micron-scale actuators, thus validating its resolution.

The actuators are powered using a two-stage amplification scheme. A signal of desired shape and frequency is generated using a Tektronix AFG3022B function generator. This signal is first stepped up for a gain of 24 using a Crown CDi4000 audio amplifier and is further amplified for a gain of 220 through a high-voltage transformer (Corona Magnetics, Inc., CMI 5523). A current probe (Pearson Electronic 2100) and a high voltage probe (Tektronix P6015A) capture the current and voltage data through a digitizing oscilloscope (Tektronix DPO2014).

The actuators are made of 40 μm adhesive backed copper strips taped to either side of a dielectric plate. The upstream edge of the powered electrode is covered with Kapton tape to prevent any reverse discharge, and the ground electrode is covered with either several layers of electrical tape, or hot glue, depending on the operating voltage. Figure 1(c) illustrates the general configuration of the actuator, and Table I provides summary details of the parameters tested.

To ensure reliability, the setup is benchmarked against published data[10] as plotted in Figure 3, which show decent qualitative agreement. However, the thrust values obtained herein are, in general, higher by 100 mg (Tt/L = 3 mN-mm/m approx.) or more. This anomaly may be due to the difference in the dielectric thickness and the dielectric material (reference actuator[10] used 1.8 mm glass-fiber-reinforced epoxy dielectric, while we used 1.58 mm Garolite grade G-10 dielectric).

Figure 4 shows the thrust and effectiveness trends for four different thicknesses of the Teflon® dielectric. For all cases, the thrust reaches a maximum at a pressure lower than the atmospheric, confirming previous observation.[10] The pressure of this maxima (P_m) decreases as the dielectric thickness decreases ($P_m = 56$ Kpa for 3.17 mm versus $P_m = 26$ kPa for 0.25 mm). The peak non-dimensionalized thrust ($T_{nd} = T/T_{atm}$) increases with decreasing thickness, suggesting an increase in thrust ranging from several percent for thicker dielectric to several-fold for thinner dielectric (76% for 3.17 mm versus 675% for 0.25 mm).

The power consumption (data not shown due to space constraints) increases at lower pressure, with thinner dielectric incurring a higher increase (300% increase for 3.17 mm thick Teflon versus 800% for 0.25 mm thick Teflon over the same pressure range).

The effectiveness (ζ) of the actuators, defined as the ratio of measured thrust and input power,[15] is found to exhibit

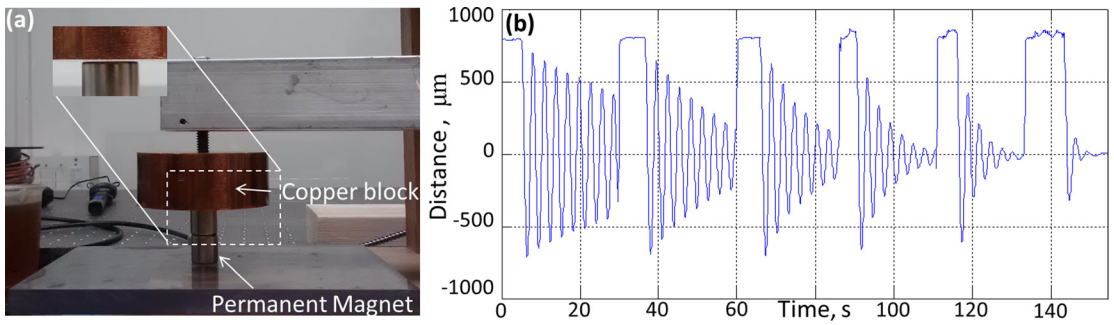

FIG. 2. (a) Details of the magnetic damper. (b) System response with increasing damping.

TABLE I. Details of the actuator geometries and operating parameters.

Setup	Dielectric	a (mm)	b (mm)	t (mm)	L (cm)	V (kVpp)	f (kHz)
Ohaus	Teflon	5	12.5	0.25 0.80 1.58 3.17	30	6 8 12 15–20	14 kHz
	Garolite[a]	15	15	1.58	12	20	5 kHz
μNTS	Kapton Teflon	5	5	0.05 0.13 0.25	4	6	14 kHz

[a]Actuator has 1 mm electrode gap to match benchmark actuator.[10]

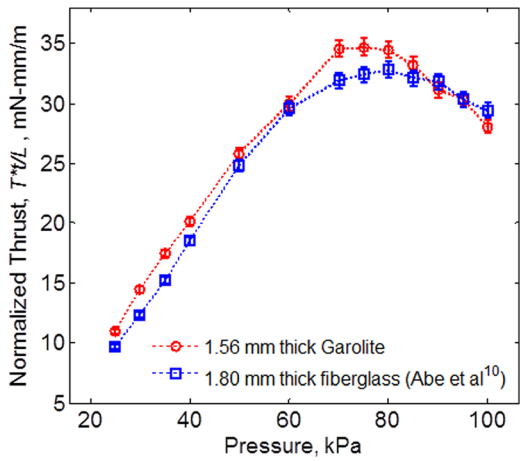

FIG. 3. Thrust vs. pressure for Garolite dielectric. 15 mm powered and ground electrodes, 1 mm electrode gap, 20 kVpp at 14 kHz. Solid (filled) marker shows projection using Eq. (3).

a local maximum. Figure 4(b) shows the relative effectiveness (effectiveness at a given pressure over effectiveness at atmospheric pressure) for the four dielectric thicknesses tested. The pressure at which the maximum occurs depends on the dielectric thickness, with thinner dielectric experiencing higher gain (10% for 3.17 mm versus 70% for 0.25 mm), reflecting the thrust trend.

Figure 5(a) shows measured thrust as a function of the background pressure for 3.17 mm thick Teflon at various operating voltages. Both the amount of increase in thrust and the pressure at which it peaks are found to be a function of the operating voltage (the maximum $T_{nd} = 1.8$ at 53 kPa for 15 kVpp, while the maximum $T_{nd} = 1.3$ at 23 kPa for 20 kVpp). Of particular interest is the 1.58 mm thick Teflon actuator operating at 12 kVpp, which is under a similar nominal electric field as the 3.17 mm Teflon operating at 20 kVpp (3.80 MV/m vs. 3.15 MV/m). The thinner dielectric of the two is found to undergo higher force amplification (220% vs. 30%), suggesting thinner dielectrics might be better suited for high-altitude/low-pressure operation.

For smaller actuators, the thrust is measured using μNTS for better resolution. The measured thrust from the μNTS agrees well qualitatively with that from the commercial balance (Figure 6). The thrust peaks at a sub-atmospheric pressure before dropping down again. The 4 cm long 0.25 mm thick Teflon dielectric is seen to undergo a similar magnitude of thrust increase (700%) as its 30 cm long counterpart. The power consumption is seen to increase as the pressure goes down, and the amount of increase is found to be higher for thinner dielectrics, consistent with the results from the Ohaus setup. The actuators have noticeably different effectiveness due to dissimilar widths of the ground electrodes (12.5 mm for Ohaus setup versus 5 mm for μNTS setup). The overall force is seen to be higher for a wider ground electrode as expected,[8] but force amplification seems to be not significantly different.

The systematic dependence of peak actuator thrust on dielectric thickness, and the pressure at which this occurs, hints towards a causal relationship. An attempt is made to capture this trend in a unified equation which relates these variables. Multivariate analysis in conjunction with curve-fitting suggests the following empirical relationships among the various parameters:

$$P_{\mathrm{m}} = 11.43E, \tag{1}$$

$$T_{\max} = 0.4e^{0.0437P_{\mathrm{m}}} + 0.585e^{0.428E}, \tag{2}$$

$$T_{\max} = 6(\varepsilon_n^{0.5})(1 - e^{-w_n^{1.25}})[0.4e^{0.0437P_{\mathrm{m}}t_n} + 0.585e^{0.428Et_n^{0.85}}]. \tag{3}$$

Here, P_m is the pressure (kPa) at which the thrust peaks, E is the nominal electric field (MV/m), T_{max} is the peak thrust per meter length (mN/m), t_n is the normalized thickness (t/t_{ref}), w_n is the normalized ground electrode width (w/w_{ref}), and ε_n is the normalized dielectric constant ($\varepsilon_r/\varepsilon_{ref}$). The reference values are $t_{ref} = 3.17$ mm, $w_{ref} = 50$ mm, $\varepsilon_{ref} = 2.1$.

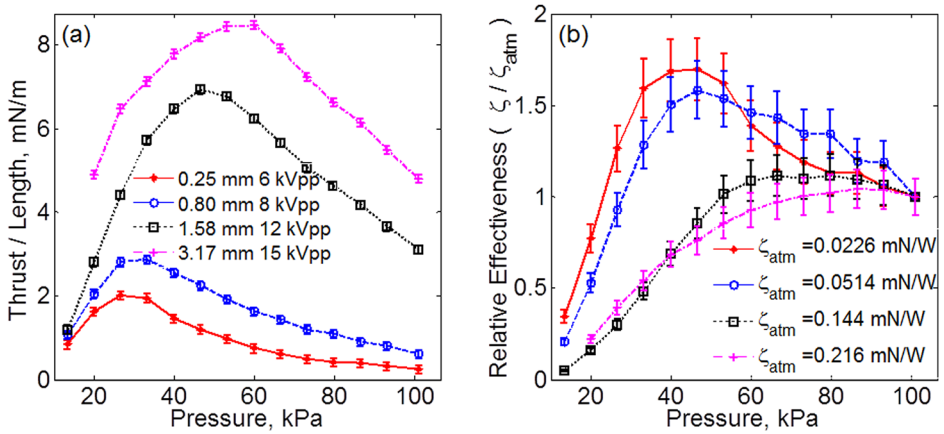

FIG. 4. (a) Thrust per length and (b) relative effectiveness for various thicknesses of Teflon dielectric (Ohaus setup).

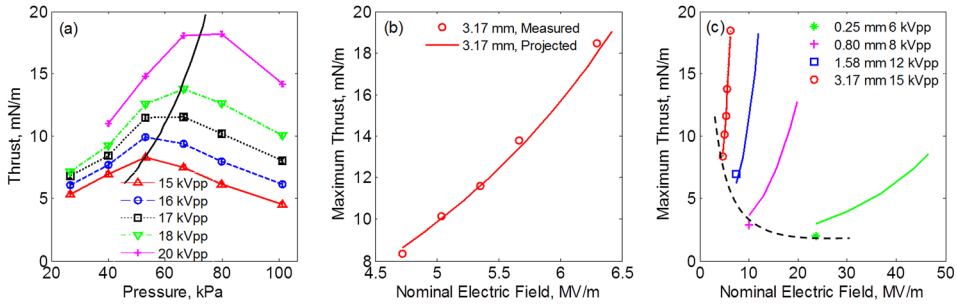

FIG. 5. (a) Thrust per length at varying voltages for 3.17 mm thick Teflon dielectric, (b) maximum thrust as a function of nominal electric field, as captured by Eq. (2), and (c) extension of this trend for various dielectric thicknesses using Eq. (3). Solid black line in (a) represents Eq. (2). Dashed black line in (c) represents approximate behavior of Eq. (3) for varying thickness. In (c), solid lines represent projections; marker locations represent experimental data.

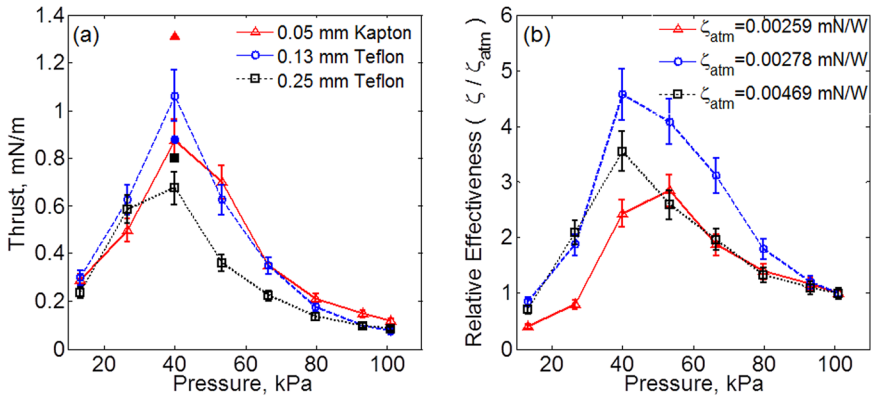

FIG. 6. Thrust per length (a), relative effectiveness (b) for μNTS setup. Actuators are powered with 6 kVpp. Solid markers indicate projections of Eq. (3).

Equation (2) is plotted in Figure 5(a) (solid black line). The curve seems to mimic the peak force trend fairly well. For a given thickness (3.17 mm), the projected values from Eq. (2) match within 5% of the measured values (Figure 5(b)). To account for variation in thickness, dielectric constant, and ground electrode width, Eq. (2) is modified by introducing the normalized quantities t_n, ε_n, and w_n (Eq. (3)). The projected values for 0.25 mm, 0.80 mm, and 1.58 mm Teflon dielectric using this revised equation (Figure 5(c)) are found to be within 16%, −4%, and −33%, respectively. Figure 3 shows the projected value for a different dielectric material, thickness, and ground electrode width (Garolite, 1.58 mm, 15 mm). The projection is within 14% of the measured value. Figure 6(a) shows similar projections (Teflon, 0.13 mm and 0.25 mm thick, 5 mm ground, and Kapton, 0.05 mm thick, 5 mm ground). The projected values are seen to be within 20% of the respective measured values, with the exception of Kapton, where Eq. (3) over-predicts the force by about 45%. This deviation can be explained considering the extremes of thickness (0.05 mm) and electric field (59 MV/m) that this actuator is under. Thrust saturation for 0.16 mm Kapton at 12 kVpp and identical frequency (14 kHz) has been reported in literature.[2] This corresponds to an electric field of approximately 36 MV/m. The electric field for the Kapton actuator in the current study is 60% higher than this value, suggesting the actuator is already operating in or beyond the thrust saturation region. Equation (3) does not account for any saturation phenomena, thus over predicting the value.

Figure 7 shows the visual extent of plasma and the current and voltage profiles for 0.25 mm Teflon dielectric at various pressures. As the pressure goes down, the discharge spikes are seen to grow slightly in magnitude and frequency (upto 67 kPa), before become shorter and sparse at lower

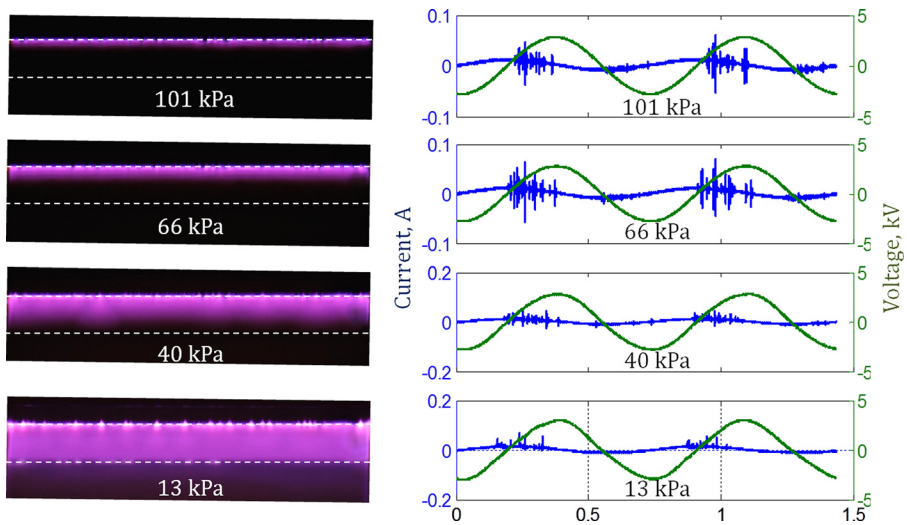

FIG. 7. Visual plasma extent (left) and current and voltage profiles (right) for 0.25 mm Teflon dielectric at 14 kHz, 6 kVpp. Dotted white lines denote extent of ground electrode (5 mm).

pressures. The phase angle at which the discharge spikes initiate also shifts towards the left as the pressure goes down. At atmospheric pressures, the spikes begin at approximately 90° into the current signal phase. However at 13 kPa, this initiation takes places upto 45° earlier in the phase. This is complimented by another observation that the diffuse discharge present during the negative half cycle at ambient pressures is nearly absent at lower pressure. This suggests that at atmospheric pressures, strong plasma is produced for the entire duration of the positive-rising voltage pulse, whereas only a weak discharge is produced during the negative-going duration of the cycle. At low pressure however (13 kPa), plasma starts forming while the voltage is still negative but rising and lasts till the voltage reaches the peak value. There is no significant discharge during rest of the cycle.

In summary, low pressure performance of DBD actuators is investigated over a pressure range of 13 to 101 kPa using a commercial balance and an indigenous high resolution thrust stand. The effects of dielectric thickness, operating voltage, and ground electrode width are investigated. The thrust is found to rise upto a certain threshold pressure before decreasing gradually to zero. The increase in thrust is found to be a strong function of dielectric thickness, with 75% increase for 3.17 mm thick Teflon to 675% for 0.25 mm thick Teflon. The pressure at which the thrust peaks is also found to be dependent on dielectric thickness. For fixed thickness, the thrust increase is found to be dependent on the operating voltage, with a 75% increase at 15 kVpp to 30% increase at 20 kVpp for 3.17 mm thick Teflon. The effectiveness exhibits a maximum at a sub-atmospheric pressure, and both the percentage increase and the pressure at which it peaks are dependent on dielectric thickness, and is seen to increase by upto 70%. For a similar nominal electric field, a thinner dielectric field is found to undergo higher thrust amplification than a thicker one. Empirical relations suggest exponential effect of dielectric thickness, electric field, and ground electrode width on the maximum actuator thrust, while the pressure at which the thrust peaks is found to be linearly proportional to the electric field. This empirical model exhibits good agreement with experimental data over a wide range of control parameters. These results open up the possibility of optimal control of plasma actuators for high altitude operations.

[1]J. R. Roth, D. M. Sherman, and S. P. Wilkinson, AIAA J. **38**, 1166–1172 (2000).
[2]R. J. Durscher and S. Roy, J. Phys. D: Appl. Phys. **45**, 012001 (2012).
[3]R. Mestiri, R. Hadaji, and S. Ben Nasrallah, Phys. Plasmas **17**, 083503 (2010).
[4]C. L. Enloe, T. E. McLaughlin, R. D. Van Dyken, K. D. Kachner, E. J. Jumper, and T. C. Corke, AIAA J. **42**(3), 589–594 (2004).
[5]C. L. Enloe, T. E. McLaughlin, R. D. Van Dyken, K. D. Kachner, E. J. Jumper, T. C. Corke, M. Post, and O. Haddad, AIAA J **42**(3), 595–604 (2004).
[6]C. L. Enloe, M. G. McHarg, and T. E. McLaughlin, J. Appl. Phys. **103**, 073302 (2008).
[7]T. C. Corke, C. L. Enloe, and S. P. Wilkinson, Annu. Rev. Fluid Mech. **42**, 505–529 (2010).
[8]F. O. Thomas, T. C. Corke, M. Iqbal, A. Kozlov, and D. Schatzman, AIAA J. **47**, 2169–2178 (2009).
[9]J. W. Gregory, C. L. Enloe, G. I. Font, and T. E. McLaughlin, 45th AIAA Aerospace Sciences Meeting and Exhibit, AIAA Paper No. 2007-0185, 2007.
[10]T. Abe, Y. Takizawa, and S. Sato, AIAA J. **46**, 2248–2256 (2008).
[11]J. A. Valerioti and T. C. Corke, AIAA J. **50**, 1490–1502 (2012).
[12]P. Versailles, V. Gingras-Gosselin, and H. Duc Vo, AIAA J. **48**, 859–863 (2010).
[13]M. Gamero-Castaño, Rev. Sci. Instrum. **74**, 4509–4514 (2003).
[14]J. C. Zito, R. J. Durcher, J. Soni, S. Roy, and D. P. Arnold, Appl. Phys. Lett. **100**, 193502 (2012).
[15]R. J. Durscher and S. Roy, 48th AIAA Aerospace Sciences Meeting, Orlando, FL, AIAA Paper No. 2010-965, 2010.